John W. Hutchinson[1] *and Viggo Tvergaard*[2]

Softening Due to Void Nucleation in Metals

REFERENCE: Hutchinson, J. W. and Tvergaard, V., **"Softening Due to Void Nucleation in Metals,"** *Fracture Mechanics: Perspectives and Directions (Twentieth Symposium), ASTM STP 1020,* R. P. Wei and R. P. Gangloff, Eds., American Society for Testing and Materials, Philadelphia, 1989, pp. 61–83.

ABSTRACT: The mechanics of void nucleation in an elastic-plastic solid stressed into the plastic range is studied with emphasis on the contribution of nucleation to softening of overall stress-strain behavior. Results for nucleation of an isolated spherical void in an infinite matrix under triaxial remote stressing are used to predict overall stress-strain behavior when interaction between voids is negligible. Calculations for nucleation of a void at a rigid spherical particle in a cylindrical cell model the simultaneous nucleation of a uniform distribution of voids. A strong dependence of the nucleation process on the matrix material specification is found when results based on isotropic hardening are contrasted with those based on kinematic hardening. At issue is the magnitude of the softening contribution due to void nucleation. This issue and the role of nucleation in promoting flow localization are discussed.

KEY WORDS: cell model, dilatation, isolated, isotropic, J_2-flow theory, kinematic hardening, macroscopic, matrix strain hardening, nucleation, plasticity, softening, strain, stress, triaxiality, void

Nucleation of voids in a plastically deforming metal has two consequences. Most obvious is the generation of damage, which ultimately will lead to failure of a ductile metal after further straining. A less obvious but equally important consequence is the reduction in macroscopic strain-hardening capacity due to the nucleation process itself, independent of the subsequent growth of the void. The shedding of the load carried by a particle when a void nucleates by interface debonding between the particle and the matrix or by particle cracking causes a redistribution of stress and strain in the matrix, which alters the overall stress-strain behavior of the material. The consequences of nucleation in offsetting matrix strain hardening can be dramatic. There is evidence that some high-strength steels undergo shear localization simultaneously, or almost simultaneously, with the onset of void nucleation at second-phase particles.

This paper focuses on the effect of void nucleation on macroscopic stress-strain behavior. We introduce the subject by displaying one set of results from a numerical calculation carried out in the section on Cell Model Calculations. An axisymmetric cell model is used to model the simultaneous nucleation of voids at a uniform distribution of rigid spherical particles. The cell, which is shown in Fig. 1, is constrained such that the ends remain planar and the lateral surface remains cylindrical. The macroscopic true stresses S and T are obtained as averages of the local normal stresses over the respective surfaces. Prior to nucleation, S and T are increased monotonically with a fixed ratio, T/S, and the distribution of stress and

[1] Professor, Division of Applied Sciences, Harvard University, Cambridge, MA 02138.
[2] Professor, Department of Solid Mechanics, The Technical University of Denmark, Lyngby, Denmark.

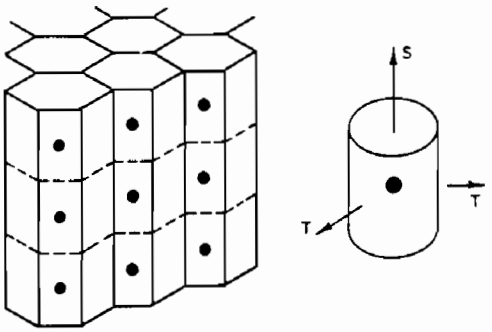

FIG. 1—*Cylindrical cell model of uniform array of void-nucleating spherical particles.*

strain in the cell is calculated. Then at a given macroscopic true stress state, the void in the cell is "nucleated" by incrementally reducing the traction across the particle/matrix interface to zero.

The overall stress-strain behavior shown in Fig. 2 was calculated for nucleation under constant S and T at two stress levels (other possibilities are analyzed in the section noted above). The horizontal segments display the amount of overall strain which occurs during nucleation. In this example, the volume fraction of the spherical particle is 1%, the stress triaxiality is $T/S = 0.5$, and the multiaxial stress dependence of the matrix material is described by J_2-flow theory. Included in Fig. 2 for reference are the stress-strain behavior in the absence of nucleation and the stress-strain behavior of the cell containing a void which at the start of straining has a 1% volume fraction. The strain following nucleation at finite stress is only slightly less than corresponding strain when the void is present from the start, and following nucleation the two curves are similarly close. By contrast, the growth in volume of the void during nucleation, ΔV, has a very strong history dependence. This can be seen in Fig. 3, where the volume growth, normalized by the particle volume V_0 and the

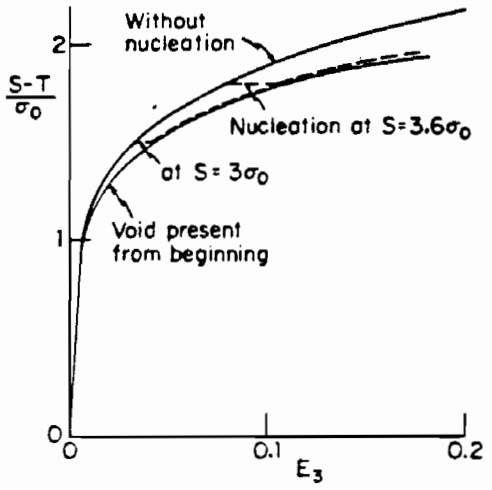

FIG. 2—*Overall stress-strain behavior for nucleation at constant stress for rigid spherical particles in a matrix material governed by J_2-flow theory* ($\rho = 0.01$, $\epsilon_0 = 0.004$, $n = 5$, $\nu = 0.3$).

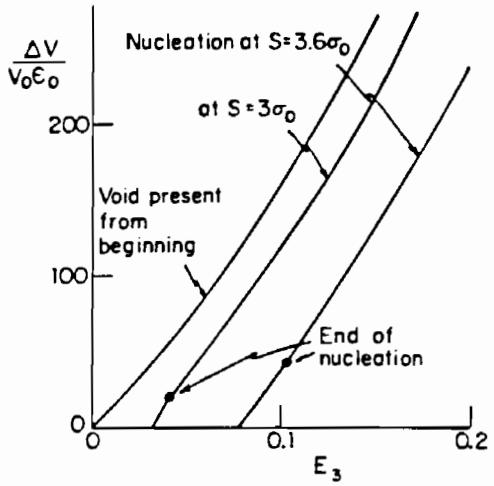

FIG. 3—*Normalized volume increase as a function of overall strain for nucleation at constant stress in a J_2-flow theory matrix.*

initial yield strain ϵ_0, is plotted as a function of the macroscopic logarithmic strain. The segment of the curve ending in the solid dot corresponds to the void growth during nucleation, which is far less than that experienced by a void present from the start.

The first part of the paper deals with the basic problem of nucleation of a spherical void in an infinite matrix under remote triaxial stressing. Application of the solution to this problem to predict the effect of nucleation on macroscopic stress-strain behavior is discussed. The second part of the paper presents an analysis of the cylindrical cell model described above. In each part, the role of the multiaxial stress characterization of the matrix material is explored by using both J_2-flow theory (isotropic hardening) and kinematic hardening. Nucleation as predicted by the Gurson model [*1*] is related to the results of the present paper in the section on Effect of Nucleation.

Nucleation of an Isolated Void and Its Effect on Macroscopic Stress-Strain Behavior

Before analyzing in detail the mechanics of void nucleation, we first outline the nature of the results expected and show how these can be used to predict the effect of void nucleation on stress-strain behavior.

Consider nucleation of a single void at a spherical particle of unit volume in an infinite matrix stressed into the plastic range by proportional application of a remote stress $\mathbf{\Sigma}$. Imagine that the interface between the particle and the matrix debonds, either partially or completely, when the remote stress reaches $\mathbf{\Sigma}$. This nucleation event causes a redistribution of stress, some growth of the void and additional straining in the matrix. Denote the average extra strain that occurs as a result of nucleation of the void, over and above what occurs in the absence of nucleation, by $\Delta\mathbf{E}$, such that $\Sigma_{ij}\Delta E_{ij}$ is the extra work done by the remote stress due to nucleation. For proportional stressing to $\mathbf{\Sigma}$, $\Delta\mathbf{E}$ is an isotropic function of $\mathbf{\Sigma}$, assuming the unstressed matrix is isotropic. Approximate results for $\Delta\mathbf{E}$ are given in the next section.

Let $\mathbf{M}$ denote the current overall (diagonally symmetric) incremental compliances of a macroscopic element of material subject to macroscopic stress $\mathbf{\Sigma}$ when no particles nucleate

voids. Thus the macroscopic strain increment is

$$\dot{E}_{ij} = M_{ijkl}\dot{\Sigma}_{kl} \tag{1}$$

in the absence of nucleation. Now suppose that during the stress increment $\dot{\boldsymbol{\Sigma}}$ voids nucleate in the material element corresponding to a volume fraction increment $\dot{\rho}$. If the nucleated voids are sufficiently widely spaced so that their interaction can be ignored (for example, $\dot{\rho}$ sufficiently small), then in the presence of nucleation

$$\dot{E}_{ij} = M_{ijkl}\dot{\Sigma}_{kl} + \dot{\rho}\Delta E_{ij} \tag{2}$$

With $\mathbf{L} = \mathbf{M}^{-1}$ as the incremental moduli of the material element in the absence of nucleation, it follows from Eq 2 that in the presence of nucleation

$$\dot{\Sigma}_{ij} = L_{ijkl}\dot{E}_{kl} - \dot{\rho}\Delta\Sigma_{ij} \tag{3}$$

where

$$\Delta\Sigma_{ij} = L_{ijkl}\Delta E_{kl} \tag{4}$$

The quantity $\dot{\rho}\Delta\boldsymbol{\Sigma}$ can be interpreted as the average stress drop due to nucleation of an increment of void volume fraction $\dot{\rho}$ relative to the stress in the absence of nucleation at the same macroscopic strain. Figure 4 displays the schematic interpretation of $\dot{\rho}\Delta\mathbf{E}$ and $\dot{\rho}\Delta\mathbf{E}$ relative to the overall stress-strain curves with and without nucleation.

The focus in this paper is on the first nucleation of voids in a void-free material, but the above discussion also applies, at least approximately, to subsequent nucleation adding to voids nucleated earlier in the stress history. Then, $\mathbf{L}$ and $\mathbf{M}$ correspond to incremental moduli and compliances in the presence of a volume fraction ρ of voids but without nucleation of additional voids $\dot{\rho}$. The extra average strain ΔE due to nucleation of the isolated void should in general account for interaction with preexisting voids.

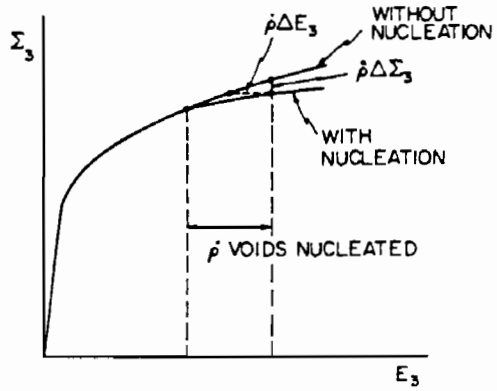

FIG. 4—*Interpretation of* $\Delta\boldsymbol{\Sigma}$ *and* $\Delta\mathbf{E}$ *in uniaxial tension.*

Extra Strain, $\Delta\mathbf{E}$, and Stress Drop, $\Delta\mathbf{\Sigma}$, Due to Nucleation of an Isolated Spherical Void

In this section the nucleation of an isolated spherical void in an infinite block of material is modeled as a mechanics problem. The solution procedure is given in the Appendix, and approximate recipes for $\Delta\mathbf{E}$ and $\Delta\mathbf{\Sigma}$ are presented in this section.

An infinite block of material is stressed into the plastic range by proportional application of remote stress $\mathbf{\Sigma}$. The void is nucleated from a fictitious "particle" which deforms uniformly with the matrix prior to nucleation. Thus at the onset of nucleation the block of material is in a uniform state of stress $\mathbf{\Sigma}$ and the "particle" is taken to be spherical with unit volume. The nucleation process is modeled as a plasticity problem in which tractions across the particle/matrix interface at the onset, $T_i^0 = \Sigma_{ij} n_j$, are incrementally reduced to zero. Specifically, traction rates, $-\dot{\lambda}_0 T_i^0$, are applied to the interface, with $\lambda_0 = 0$ coinciding with the onset of nucleation and $\lambda_0 = 1$ with completion. The tractions on the interface are reduced to zero quasi-statically and uniformly. In many instances, the actual debonding process is likely to involve a dynamic interfacial separation by progressive cracking, which is not modeled here. A more detailed treatment of the debonding process is given by Needleman [2]. Contact between the "particle" and the nucleating void is ignored, but does not occur in any case in which the remote stress has modest triaxiality. We consider also the possibility that the nucleation process occurs under proportionally increasing remote stress $\dot{\lambda}_\infty \mathbf{\Sigma}$ simultaneously with traction-rates $-\dot{\lambda}_0 T_i^0$ on the interface.

The void nucleation problem just described is a small strain plasticity problem. The sequence of incremental problems in the void nucleation process does not lead to either large geometry changes of the void or large strain changes anywhere in the material surrounding the void. For our purposes here we take the hardening level in the matrix, as measured by the tangent modulus E_t of the effective stress-strain curve, to be constant during nucleation. In doing so, it is imagined that the strain changes during nucleation are small compared to the strain at the onset of nucleation such that only very small changes in E_t would occur during nucleation, and these are neglected. Results will be presented for both J_2-flow theory (isotropic hardening) and kinematic hardening to give some indication of how strongly the predictions are influenced by the matrix material description. Some influence is certainly expected since the stress changes in the vicinity of the void which occur during nucleation are distinctly nonproportional, and thus the material characterized by isotropic hardening should offer more resistance to plastic straining than the kinematic hardening material.

Let σ_0 be the initial tensile yield stress of the material, E its Young's modulus, and $\epsilon_0 = \sigma_0/E$ the tensile strain at initial yield. For computational convenience, we have taken the material to be incompressible. For J_2-flow theory the increment in the stress deviator, s, is

$$\dot{s}_{ij} = \frac{2}{3} E\dot{\epsilon}_{ij} - (E - E_t)s_{ij}s_{kl}\dot{\epsilon}_{kl}/\sigma_e^2 \tag{5}$$

for loading ($\sigma_e = (\sigma_e)_{\max}$ and $s_{kl}\dot{\epsilon}_{kl} \geq 0$) and

$$\dot{s}_{ij} = \frac{2}{3} E\dot{\epsilon}_{ij} \tag{6}$$

for elastic unloading. Here $\sigma_e = (3s_{ij}s_{ij}/2)^{1/2}$ is the effective stress and, as already mentioned, E_t is the tangent modulus associated with the remote stress state $\mathbf{\Sigma}$. For kinematic hardening theory based on the shifted J_2-invariant, yield is specified by $(3\hat{s}_{ij}\hat{s}_{ij}/2)^{1/2} = \sigma_0$ where $\hat{s} =$

$s - \alpha$ and α is the deviator specifying the center of the yield surface. For plastic loading ($\hat{s}_{ij}\dot{\epsilon}_{ij} > 0$),

$$\dot{s}_{ij} = \frac{2}{3} E\dot{\epsilon}_{ij} - (E - E_t)\hat{s}_{ij}\hat{s}_{kl}\dot{\epsilon}_{kl}/\sigma_0^2 \tag{7}$$

and

$$\dot{\alpha}_{ij} = E_t\hat{s}_{ij}\hat{s}_{kl}\dot{\epsilon}_{kl}/\sigma_0^2 \tag{8}$$

while Eq 6 holds for elastic increments with $\dot{\alpha} = 0$.

The remote stressing is taken to be axisymmetric with respect to the 3-axis such that the nonzero components of Σ are

$$\Sigma_{33} = S, \quad \Sigma_{22} = \Sigma_{11} = T \tag{9}$$

Denote the remote mean and effective stresses by Σ_m and Σ_e so that

$$\Sigma_m = \frac{1}{3}(S + 2T) \text{ and } \Sigma_e = |S - T| \tag{10}$$

Let δE_N denote the increase in the remote axial strain component E_{33} which is prescribed to occur during the nucleation process (that is, the strain change associated with $\dot{\lambda}_N\Sigma$). The solution procedure is given in the Appendix. The results of the calculations are now reported.

J_2-*Flow Theory Results*

We begin by an example in Fig. 5 based on J_2-flow theory which shows the evolution during nucleation of both the total dilatation of the void, ΔE_{kk}^T, and the dilatation just due to nucleation, ΔE_{kk}, for three different choices of $\delta E_N/\epsilon_0$ where $\epsilon_0 = \sigma_0/E$ is the elastic strain at yield. The dilatation due to nucleation, ΔE_{kk}, is the total dilatation with the contribution due to δE_N (that is, due to $\dot{\lambda}_N\Sigma$) subtracted off. Note that ΔE_{kk} is essentially independent of δE_N and thus is, indeed, meaningfully identified as the contribution due to nucleation. The normalized quantities $\Delta E_{kk}^T/(\Sigma_m/E)$ and $\Delta E_{kk}/(\Sigma_m/E)$ are also found to be essentially independent of Σ_m/E and of E_t/E when it is small (that is, $E_t/E < 0.1$); they do, however, depend on triaxiality, $X \equiv \Sigma_m/\Sigma_e$, as shown below.

The significance of considering different values of δE_N is that, in an actual nucleation process, this value is determined by the mechanism of debonding together with the way in which the external loading is applied. Since no particular debonding mechanism is studied here, the relevant value of δE_N cannot be determined. Therefore it is of interest to extract the part of the macroscopic behavior that is essentially independent of δE_N.

An important feature of the process is the relatively small dilatation due to nucleation. Were the process a linearly elastic one (in an incompressible elastic matrix), then

$$\Delta E_{kk} = (9/4)\Sigma_m/E \tag{11}$$

The dilatation contribution ΔE_{kk} at the end of nucleation in Fig. 5 is only about twice this elastic value. This feature stems from the distinctly nonproportional stressing in the vicinity of the void during nucleation and the resistance of the material to plastic deformation needed to enlarge the void. By contrast, if the void were nucleated this way in a nonlinear elastic material (for example, a J_2-deformation theory material), its enlargement would be inde-

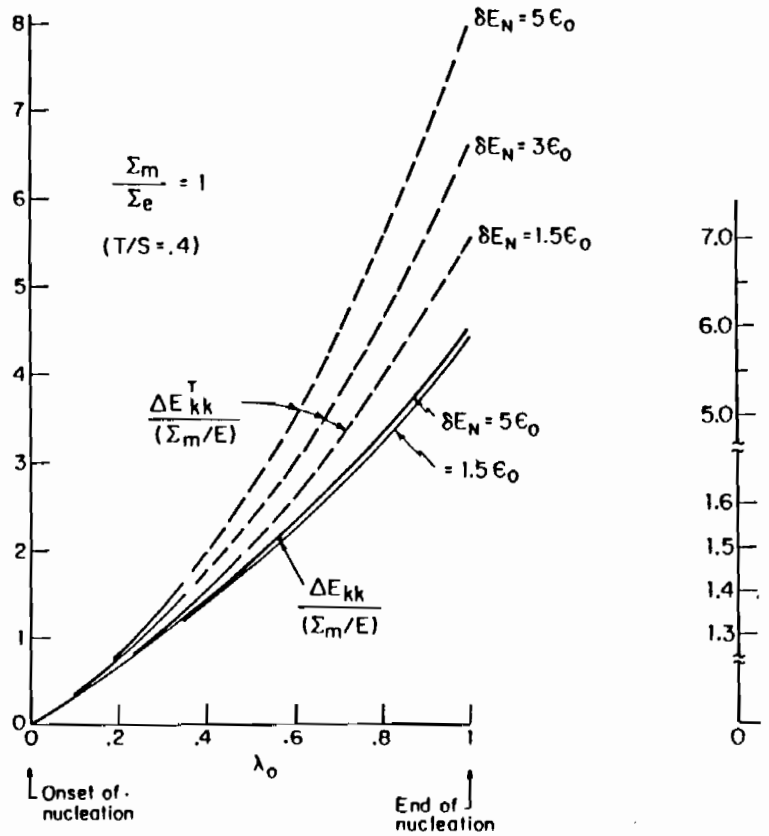

FIG. 5—*Normalized dilatation contribution for nucleation of a spherical void in an infinite matrix governed by* J_2*-flow theory* ($E_t/E = 0.02$, $S/\sigma_0 = 5$).

pendent of the history and would depend strongly on the strain at nucleation. The present results for the dilatation are essentially independent of prior plastic strain.

The deviatoric part of ΔE is much larger than the dilatation resulting from a redistribution of stress and strain throughout the matrix. It is inversely proportional to E_t rather than E. Given that ΔE must have an isotropic dependence of $\boldsymbol{\Sigma}$, we write for the contribution due just to nucleation

$$\Delta E_{ij} = F(X)\Sigma'_{ij}/E_t + G(X)\Sigma_m\delta_{ij}/E \tag{12}$$

where $\boldsymbol{\Sigma}'$ is the deviator of $\boldsymbol{\Sigma}$, $\Sigma_m = \frac{1}{3}\Sigma_{kk}$, $\Sigma_e = (3\Sigma'_{ij}\Sigma'_{ij}/2)^{1/2}$ and $X = \Sigma_m/\Sigma_e$. For axisymmetric stressing with $S \geq T$, Eq 12 is a general representation of the stress dependence, but under general remote stressing Eq 12 will only be valid if one can neglect dependence on the third invariant of $\boldsymbol{\Sigma}$ and on $\Sigma'_{ip}\Sigma'_{pj}$. The functions F and G also depend implicitly on E_t/E and δE_N, but our numerical calculations indicate that they vary by less than 2% for E_t/E in the range from 0.01 to 0.1. Figure 6 displays the dependence of F and G on δE_N for the case $X = 1$ ($T = 0.4S$). The results for the triaxiality dependence of F and G shown in Fig. 7 are computed with $\delta E_N/\epsilon_0 = 10$, but as seen in Fig. 6, the dependence on δE_N is very weak. Included in Fig. 7 are predictions for F which derive from the Gurson [*1*] model, which will be discussed in the section on Effect of Nucleation.

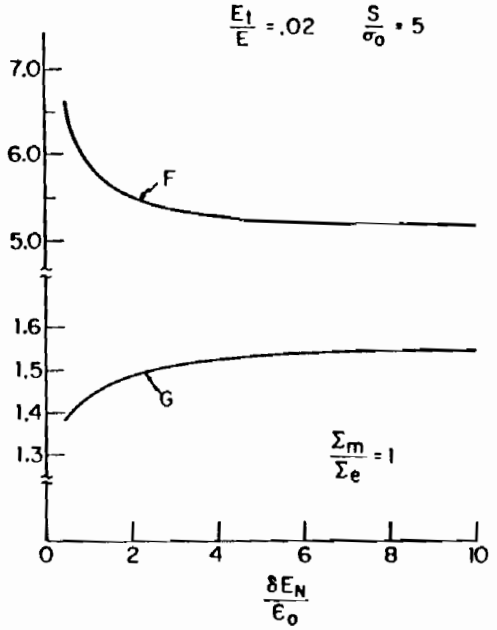

FIG. 6—*Dependence of* F *and* G *on* $\delta E_N/\epsilon_0$ *for nucleation in a matrix governed by* J_2*-flow theory.*

As mentioned earlier, interaction between the "particle" and the void surface is ignored in the calculations once nucleation starts. Inspection of the numerical solution indicates that the void surface pulls away from the particle at every point if $T/S > 0.1$ and δE_N is not large. Thus, only the values of F and G at very low triaxialities ($X < 0.44$) would be changed by a calculation which accounted for constraint of the particle on the void deformation.

Kinematic Hardening Results

For proportional stressing histories, the two plasticity theories (Eqs 5 and 7) coincide, but the isotropic hardening material offers more resistance to plastic flow under nonproportional histories than does its kinematic counterpart. As already mentioned, the nucleation process involves distinctly nonproportional stressing near the void, and thus it is expected that the curvature of the yield surface will affect ΔE.

The calculations of F and G were repeated using the kinematic hardening description of the matrix material, Eqs 6 to 8. In this case, there is a strong dependence on $Y = \Sigma_e/\sigma_0$ as well as on the triaxiality measure $X = \Sigma_m/\Sigma_e$. For kinematic hardening Eq 12 is rewritten as

$$\Delta E_{ij} = F(X,Y)\Sigma'_{ij}/E_i + G(X,Y)\Sigma_m\delta_{ij}/E \tag{13}$$

Plots of F and G as functions of X are shown in Fig. 8 for three levels of $Y = \Sigma_e/\sigma_0$. For Y just above unity, corresponding to nucleation before the material hardens appreciably, the results for kinematic hardening are only slightly larger than those for isotropic hardening, as would be expected. For nucleation at larger values of Y, the strain contribution ΔE predicted by the kinematic theory is significantly larger than the isotropic hardening result, by factors as much as two or three.

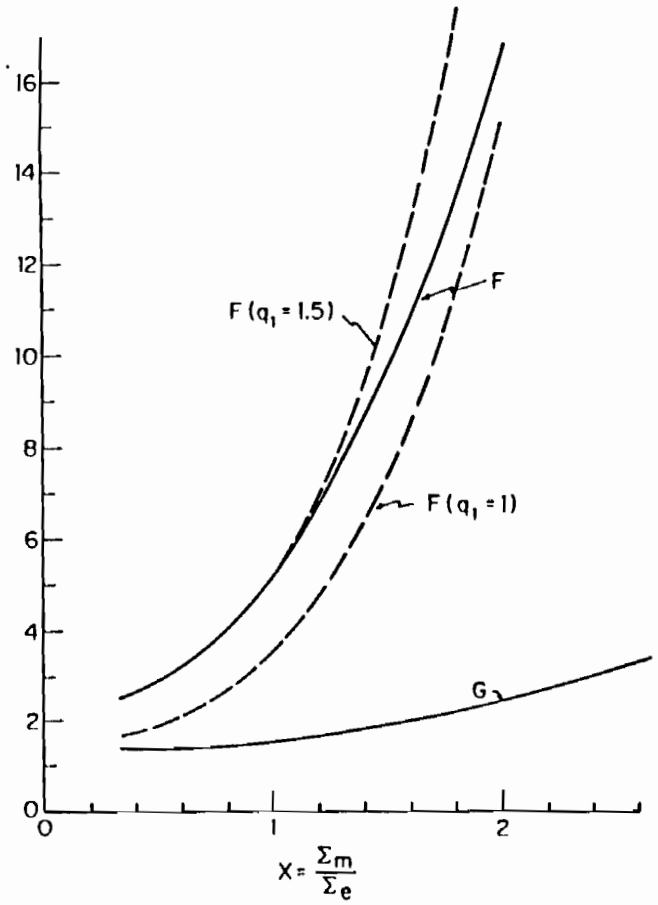

FIG. 7—*Dependence of* F *and* G *on triaxiality for matrix material governed by* J_2*-flow theory.*

As will be even clearer from the cell model results in the next section, the enhancement of the strain produced by nucleation in a kinematic hardening material over that in an isotropic hardening material is a major effect. In other problem areas, such as plastic instability phenomena, where there are significant differences between the predictions based on these two material models, the isotropic hardening model invariably tends to be overly stiff compared with experimental observations. The issue here is not fully reversed loading and Bauschinger effects; rather, it is continued loading under nonproportional stress histories. The kinematic theory reflects, albeit crudely, the high curvature or possibly even a corner, which develops at the loading point of the subsequent yield surface.

To calculate $\Delta\boldsymbol{\Sigma}$ defined by Eq 4, assume that $\Delta\mathbf{E}$ is given approximately by Eq 12 or 13 even when Poisson's ratio ν is not ½. Then by Eqs 4 and 12, one obtains

$$\Delta\Sigma_{ij} = \frac{2}{3} F\Sigma'_{ij} + \frac{1}{1 - 2\nu} G\Sigma_m\delta_{ij} \tag{14}$$

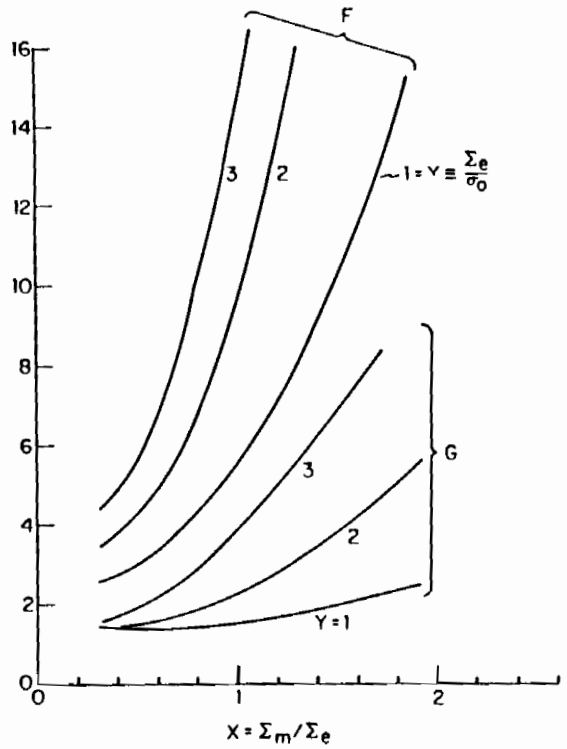

FIG. 8—*Dependence of* F *and* G *on triaxiality and* Σ_e/σ_0 *for matrix material governed by kinematic hardening theory.*

when $E_t \ll E$. This result also holds for kinematic hardening with the respective F and G values. The dilatational part of the stress drop due to nucleation at a given macroscopic strain necessarily becomes ill-defined for an incompressible matrix material.

Cell Model Calculations of Overall Stress-Strain Behavior as Influenced by Void Nucleation

The effect of a uniform distribution of spherical particles that nucleate voids simultaneously is studied by numerical solution of the axisymmetric model problem illustrated in Fig. 1. Here, the particles are assumed to be rigid, which means that in contrast to the calculation in the previous section, the stress state in the matrix material is not uniform prior to nucleation. As in the previous calculations, nucleation is simply modeled by releasing the displacements of the matrix material on the particle-matrix interface and incrementally reducing the corresponding surface tractions to zero.

Finite strains are accounted for in these cell model calculations. A Lagrangian formulation of the field equations is used, with reference to a cylindrical coordinate system, in which x^1 is the radius, x^2 is the circumferential angle, and x^3 is the axial coordinate. The displacement components on the reference base vectors are denoted u^i, where $u^2 \equiv 0$ by the assumption

of axisymmetry. The Lagrangian strains are given by

$$\eta_{ij} = \frac{1}{2}\left(u_{i,j} + u_{j,i} + u^k_{,i}u_{k,j}\right) \tag{15}$$

where $(\ )_{,i}$ denotes covariant differentiation in the reference configuration. The contravariant components τ^{ij} of the Kirchhoff stress tensor on the deformed base vectors are related to the Cauchy stress tensor σ^{ij} by

$$\tau^{ij} = \sqrt{G/g}\,\sigma^{ij} \tag{16}$$

where g and G are the determinants for the metric tensors g_{ij} and G_{ij} in the reference configuration and the current configuration, respectively.

The finite strain generalization of J_2-flow theory used here has been discussed in detail in Ref *3*. The incremental stress-strain relationship is of the form

$$\dot{\tau}^{ij} = L^{ijkl}\dot{\eta}_{kl} \tag{17}$$

with the tensor of instantaneous moduli given by

$$L^{ijkl} = \frac{E}{1+\nu}\left\{\frac{1}{2}\left(G^{ik}G^{jl} + G^{il}G^{jk}\right) + \frac{\nu}{1-2\nu}G^{ij}G^{kl} - \beta\,\frac{3}{2}\,\frac{E/E_t - 1}{E/E_t - (1-2\nu)/3}\,\frac{s^{ij}s^{kl}}{\sigma_e^2}\right\} - \frac{1}{2}\left\{G^{ik}\tau^{jl} + G^{jk}\tau^{il} + G^{il}\tau^{jk} + G^{jl}\tau^{ik}\right\} \tag{18}$$

Here, the value of β is 1 or 0 for plastic yielding or elastic unloading, respectively, and the tangent modulus E_t is the slope of the uniaxial true stress versus natural strain curve at the stress level σ_e. The uniaxial stress-strain behavior is represented by a piecewise power law

$$\epsilon = \begin{cases} \dfrac{\sigma}{E}, & \text{for } \sigma \le \sigma_0 \\[2ex] \dfrac{\sigma_0}{E}\left(\dfrac{\sigma}{\sigma_0}\right)^n, & \text{for } \sigma > \sigma_0 \end{cases} \tag{19}$$

where σ_0 is the uniaxial yield stress and n is the strain-hardening exponent. The values of these parameters are taken to be $\sigma_0/E = 0.004$ and $n = 5$, and, furthermore, elastic compressibility is accounted for, taking Poisson's ratio $\nu = 0.3$.

The finite strain generalization of kinematic hardening theory is analogous to the above equations. The full formulation has been given in Ref *4* and will not be repeated here.

In the numerical solution, equilibrium is based on the incremental principle of virtual work, and the boundary conditions, specified in terms of the nominal surface tractions T^i,

are

$$\dot{u}^3 = 0, \quad \dot{T}^1 = \dot{T}^2 = 0, \quad \text{at } x^3 = 0 \tag{20}$$

$$\dot{u}^3 = \dot{U}_{\text{III}}, \quad \dot{T}^1 = \dot{T}^2 = 0, \quad \text{at } x^3 = B_0 \tag{21}$$

$$\dot{u}^1 = \dot{U}_{\text{I}}, \quad \dot{T}^2 = \dot{T}^3 = 0, \quad \text{at } x^1 + A_0 \tag{22}$$

$$\left.\begin{array}{l} \dot{u}^i = 0 \text{ before nucleation} \\ \dot{T}^i = 0 \text{ after nucleation} \end{array}\right\} \quad \text{at } (x^1)^2 + (x^3)^2 = R_0^2 \tag{23}$$

The two constants $\dot{U}_{\text{I}}$ and $\dot{U}_{\text{III}}$ are displacement increments, and the ratio $\dot{U}_{\text{I}}/\dot{U}_{\text{III}}$ is calculated in each increment such that there is a fixed prescribed ratio between the macroscopic true stresses T and S (see also Ref 5).

The initial geometry of the region analyzed is shown in Fig. 9, where R_0 is the inclusion radius, A_0 is the initial radius of the cylindrical body analyzed, and $2B_0$ is the inclusion spacing along the cylinder axis. In the cases analyzed, the initial geometry is specified by $B_0/A_0 = 1$ and $R_0/A_0 = 0.2466$, corresponding to a volume fraction 0.01 of particles. The mesh used for the finite element solutions is shown in the figure, where each quadrilateral consists of four triangular elements.

Figure 2 shows the stress $(S - T)/\sigma_0$ versus the average axial logarithmic strain E_3 for two cases, where nucleation takes place under constant macroscopic stress, at $S = 3.0\sigma_0$ and $S = 3.6\sigma_0$, respectively, while $T/S = 0.5$. The matrix material follows J_2-flow theory. For comparison, the behavior of matrix material with the bonded rigid particle without nucleation and the behavior when the void is present from the beginning are also shown in the figure. Prior to nucleation, the macroscopic stress-strain curve with a rigid particle differs from that of the matrix material by less than 1%. After nucleation the stress level for a given value of the strain E_3 is nearly reduced to the level found when the void is present from the beginning. Figure 3 shows the corresponding growth ΔV of the void after nucleation,

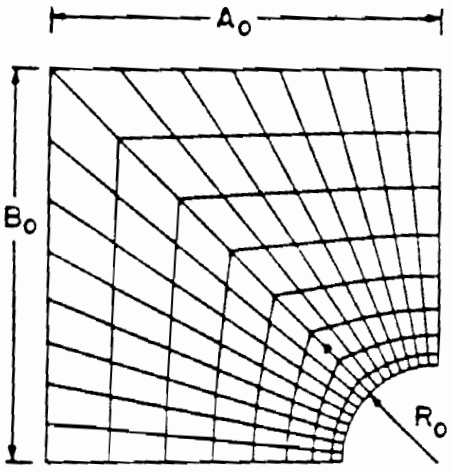

FIG. 9—*Initial geometry and finite-element grid for cylindrical cell model.*

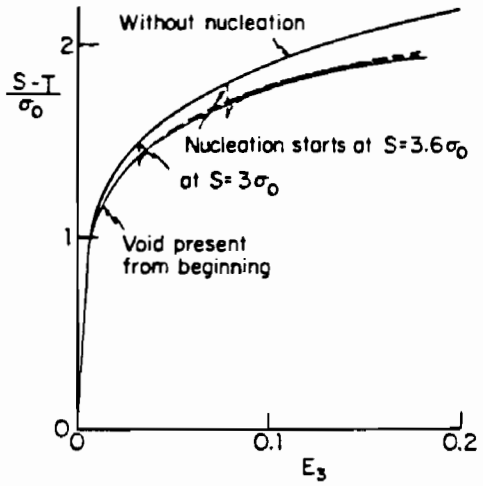

FIG. 10—*Overall stress-strain behavior for nucleation at constant strain from rigid spherical particles in a matrix material governed by J_2-flow theory* ($\rho = 0.01$, $\epsilon_0 = 0.004$, $n = 5$, $\nu = 0.3$).

normalized by the particle volume V_0 and the initial yield strain $\epsilon_0 = \sigma_0/E$. The solid dot on two of the curves indicates the point where nucleation is completed (that is, the tractions on the particle-matrix interface have been relaxed to zero). At these positions the growth is far less than that of a void present from the beginning.

Figures 10 and 11 show the same computations repeated with the only difference that here nucleation takes place under a constant macroscopic axial strain E_3, but still such that the stress ratio $T/S = 0.5$ remains constant. Here the macroscopic stresses decay during nucleation, to values somewhat below the curve for a void present from the beginning, and simultaneously a great deal of elastic unloading occurs in the matrix material near the voids. However, after some subsequent stretching these unloading regions disappear, and the

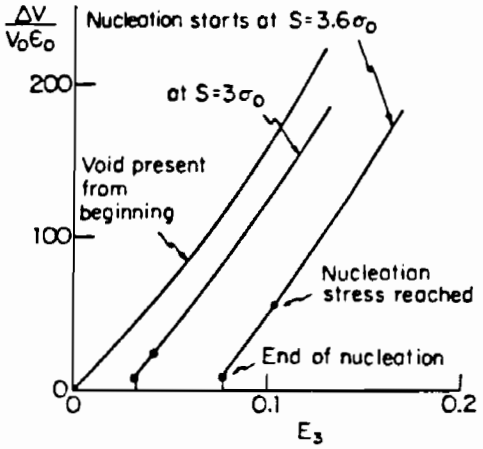

FIG. 11—*Normalized volume increase as a function of overall strain for nucleation at constant strain in a J_2-flow theory matrix.*

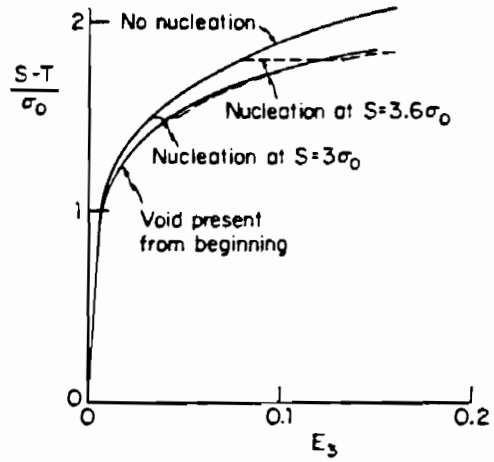

FIG. 12—*Overall stress-strain behavior for nucleation at constant stress from rigid spherical particles in a matrix material governed by kinematic hardening theory* ($\rho = 0.01$, $\epsilon_0 = 0.004$, $n = 5$, $\nu = 0.3$).

strains at which the macroscopic stress for the onset of nucleation is reached again are nearly identical to those at the end of nucleation in Figs. 2 and 3.

Kinematic hardening theory has been used to analyze the same cases, as illustrated in Figs. 12–15. Clearly, kinematic hardening has a strong influence on the predictions in the present cases, as would be expected based on Fig. 8, since the material has high hardening and the relevant values of Σ_e/σ_0 are 1.5 and 1.8, respectively. Figures 12 and 13 show that the stress-strain curves after nucleation remain below that corresponding to a void present from the beginning, in contrast to the behavior found for J_2-flow theory. Thus, the mac-

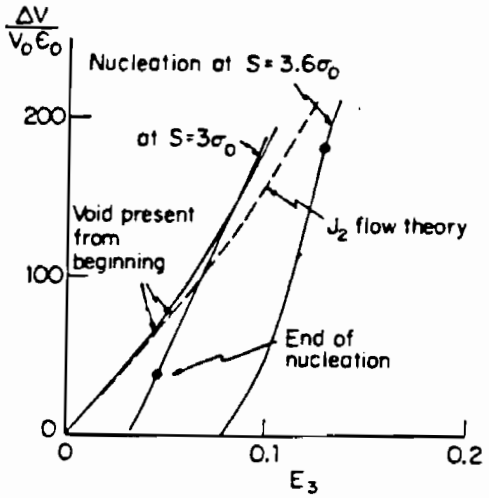

FIG. 13—*Normalized volume increase as a function of overall strain for nucleation at constant stress in a matrix material governed by kinematic hardening theory. For reference, the prediction for a matrix governed by J_2-flow theory is included as a dashed line curve for the case when the void is present from the start of straining.*

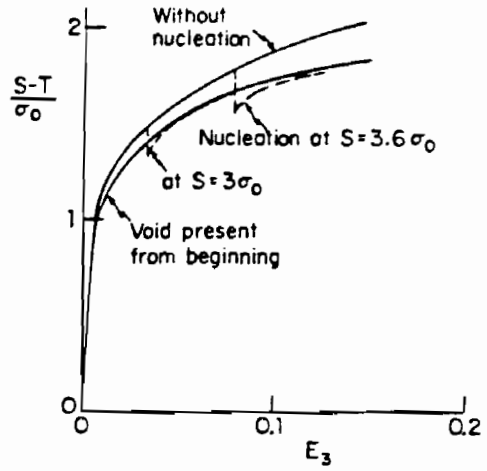

FIG. 14—*Overall stress-strain behavior for nucleation at constant strain from rigid spherical particles in a matrix material governed by kinematic hardening theory* ($\rho = 0.01$, $\epsilon_0 = 0.004$, $n = 5$, $\nu = 0.3$).

roscopic strain increment resulting from nucleation is significantly larger according to kinematic hardening theory. Figures 13 and 15 show that kinematic hardening also predicts a larger void growth during nucleation. For completeness, the comparison between the dilatation predicted by the two matrix hardening rules is included in Fig. 13 for the case in which the void is present from the start of straining. Initially, there is essentially no difference between the two predictions since the straining is everywhere nearly proportional; however, the two sets of predictions diverge as straining progresses due to nonproportionality associated with the finite expansion of the void.

The results for ΔE_{ij} obtained by these cell model calculations may be compared with Eq 2, using Eqs 12 and 13. Here, $\dot{E}_{ij}$ are interpreted as logarithmic strain increments, and $\dot{\Sigma}_{ij}$ are interpreted as true stress increments. The computations illustrated in Figs. 2 and 12 are

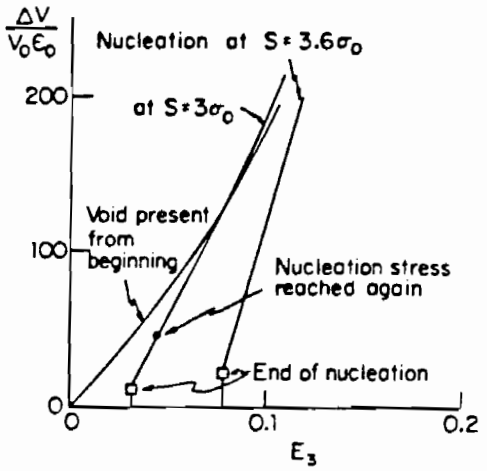

FIG. 15—*Normalized volume increase as a function of overall strain for nucleation at constant strain in a matrix material governed by kinematic hardening theory.*

most conveniently used for this comparison, since here $\dot{\Sigma}_{ij} = 0$ during nucleation. Then, with $T/S = 0.5$ prescribed in all the calculations, $\Sigma_m/\Sigma_e = 4/3$ is constant, and the values of Σ_e/σ_0 at nucleation are either 1.5 or 1.8 in the cases considered. Table 1 shows the values of ΔE_3 and ΔE_1 obtained by the cell model computations, according to Eq 2 with $\dot{\rho} = 0.01$, and the values of the functions F and G computed from Eqs 12 and 13.

The two J_2-flow theory calculations give values of F that are not too much higher than the value $F = 8.0$ given in Fig. 7, whereas the values found for G are significantly larger than the value 1.7. The results found for kinematic hardening agree qualitatively with Fig. 8, since both F and G are increased relative to the J_2-flow theory results. For the lower stress level, $\Sigma_e/\sigma_0 = 1.5$, the increases are of the same order of magnitude as those found in Fig. 8. For the larger stress level $\Sigma_e/\sigma_0 = 1.8$, the values of both F and G are much higher than those in Fig. 8.

For the values of F and G calculated by the cell model, it should be noted that the volume fraction increment $\dot{\rho} = 0.01$ is rather large. The value of the tangent modulus E_t in Eqs 12 and 13 is taken to be that of uniformly stressed matrix material at the stress level corresponding to the onset of nucleation; but due to the power-hardening relation (Eq 19) used here, this will only give a good approximation for small values of $\dot{\rho}$. The accuracy is least good for kinematic hardening at the higher stress level $\Sigma_e/\sigma_0 = 1.8$, since here the maximum stress-carrying capacity is nearly reached at the point where nucleation ends.

Effect of Nucleation as Predicted by the Gurson Isotropic Hardening Model

A prototype constitutive relation modeling void nucleation and growth has been proposed by Gurson [*1*], and this model is probably the most complete and widely used model of its type. Gurson's theory is endowed with a yield condition, a flow law, a measure of void volume fraction, a rule for nucleating voids, and a law for evolution of the void volume fraction. Its yield surface was derived from approximate solutions to a volume element of perfectly-plastic material containing a void, and it was extended to strain-hardening materials under the assumption of isotropic hardening. The stress-strain behavior of the void-free material is part of the specification of the model. With no voids present the model reduces to the classical isotropic hardening theory based on the von Mises invariant, J_2-flow theory.

Here the main equations governing the Gurson model will be briefly stated, and the quantity ΔE introduced in the section on Nucleation of an Isolated Void will be identified. We will also attempt to bring out the effect of nucleation on macroscopic strain behavior as predicted by the model. A more complete specification of the model can be found in the papers by Saje, Pan, and Needleman [*6*] and Needleman and Rice [*7*], who particularly emphasize the role of nucleation in offsetting strain hardening and in promoting flow localization.

TABLE 1—*Values of* F *and* G *computed using the cell model for* ΔE_3 *and* ΔE_1.

	ΔE_3	ΔE_1	X	Y	E_t/E	F	G
Fig. 2	0.973	−0.446	4/3	1.5	0.0395	9.3	3.4
Fig. 2	2.62	−1.22	4/3	1.8	0.0191	10.2	6.3
Fig. 12	1.391	−0.614	4/3	1.5	0.0395	13.2	6.8
Fig. 12	5.55	−2.37	4/3	1.8	0.0191	20.9	28.4

Gurson's yield function involves two material state parameters, the void volume fraction ρ and a measure of the current flow stress of the matrix material σ. With $\mathbf{\Sigma}$ as the macroscopic stress and with $\mathbf{\Sigma}'$, Σ_m and Σ_e defined as before, the yield condition is

$$\Phi(\mathbf{\Sigma}, \sigma, \rho) = \left(\frac{\Sigma_e}{\sigma}\right)^2 + 2q_1\rho \cosh\left(\frac{3q_2}{2}\frac{\Sigma_m}{\sigma}\right) - 1 - q_1^2\rho^2 = 0 \tag{24}$$

The factors q_1 and q_2 were introduced in Ref *8* to bring the yield function into better agreement with numerical results for periodic arrays of spherical voids. Gurson's original proposal employed $q_1 = q_2 = 1$, while the suggestion in Ref *8* was $q_1 = 3/2$ and $q_2 = 1$. See Ref *5* for a discussion of the current status of the yield function in comparison with experimental data and micro-mechanical calculations.

In addition to the yield condition, the following equations are postulated for plastic loading

$$\dot{E}_{ij}^p = \dot{\lambda}\partial\Phi/\partial\Sigma_{ij} \tag{25}$$

$$\Sigma_{ij}\dot{E}_{ij}^p = (1 - \rho)\sigma\dot{\sigma}[1/E_t(\sigma) - 1/E] \tag{26}$$

$$\dot{\rho} = \dot{\rho}_{\text{growth}} + \dot{\rho}_{\text{nucleation}} \tag{27}$$

$$\dot{\rho}_{\text{growth}} = (1 - \rho)\dot{E}_{kk}^p \tag{28}$$

$$\dot{\rho}_{\text{nucleation}} = A(\sigma, \Sigma_m)\dot{\sigma} + B(\sigma, \Sigma_m)\dot{\Sigma}_m \tag{29}$$

Normality is invoked in Eq 25; the condition for continued yielding, $\dot{\Phi} = 0$, allows one to determine $\dot{\lambda}$ as

$$\dot{\lambda} = \sigma\left(\frac{1}{E_t} - \frac{1}{E}\right)\left(\frac{\partial\Phi}{\partial\Sigma_{ij}}\dot{\Sigma}_{ij} + \dot{\rho}\frac{\partial\Phi}{\partial\rho}\right) \div \left(-\frac{\partial\Phi}{\partial\sigma}\frac{\partial\Phi}{\partial\Sigma_{mn}}\Sigma_{mn}\right) \tag{30}$$

Equation 26 equates the macroscopic plastic work rate to the plastic work rate in the matrix, where $E_t(\sigma)$ is the tangent modulus of the effective stress-strain curve of the matrix at σ. Equation 27 separates the increase in void volume fraction into a contribution due to growth of previously nucleated voids (Eq 28) and a contribution due to nucleation of new voids (Eq 29). Several nucleation rules of the form (Eq 29) have been proposed [6,7], but will not be detailed here.

The strain contribution due to nucleation, $\dot{\rho}\Delta E_{ij}$ in Eq 2, as predicted by the Gurson model is readily determined from the foregoing equations. For the first voids nucleated (when $\rho = 0$) at $\mathbf{\Sigma}$, the result for the void of unit volume is

$$\Delta E_{ij} = \frac{3}{2}q_1\frac{1}{E_t}\cosh\left(\frac{3q_2}{2}\frac{\Sigma_m}{\Sigma_e}\right)\Sigma_{ij}' \tag{31}$$

assuming $E_t \ll E$. Thus, when cast in the form of Eq 12, the Gurson model gives

$$F = \frac{3}{2}q_1\cosh(3q_2X/2) \text{ and } G = 0 \tag{32}$$

and this prediction is compared with the isotropic hardening results in Fig. 7 using both $q_1 = \frac{1}{2}$ and $q_1 = 1$, in each case with $q_2 = 1$. The absence of any dilatational contribution ($G = 0$) at first nucleation is a consequence of the normality assumption (Eq 25) invoked for the model. While not strictly correct, the dilatational contribution derived in the section on Nucleation of an Isolated Void is generally much smaller than the deviatoric contribution.

Nucleation is included in the Gurson model in a highly coupled manner. The quantitative effects of nucleation on macroscopic behavior are not transparent in the model. The fact that the model is in good agreement with the micro-mechanical calculation of ΔE for isotropic hardening lends confidence to the model.

The effect of nucleation as specified by the Gurson model is transparent in the case of pure shear. Since $\Sigma_m = 0$ in pure shear, the change in ρ is due entirely to nucleation. With Σ_{12} as the macroscopic shear stress and with $\tau \equiv \sigma/\sqrt{3}$ as the equivalent shear stress in the matrix material, the yield condition (Eq 24) implies (with $q_1 = 1$)

$$\Sigma_{12} = (1 - \rho)\tau \tag{33}$$

Then, with

$$\dot{\gamma}^p \equiv \sqrt{3}\dot{\epsilon}^p = \sqrt{3}\dot{\sigma}(1/E_t - 1/E)$$

as the equivalent shear strain rate in the matrix, Eqs 26 and 33 give the macroscopic shear strain rate as simply

$$2\dot{E}^p_{12} = \dot{\gamma}^p$$

independent of ρ. Thus the relation between the macroscopic shear stress-strain curve and the corresponding matrix curve is exceptionally simple as sketched in Fig. 16. The relation between Σ_{12} and E^p_{12} depends only on the current value of ρ, independent of when the voids have been nucleated.

Under other stress histories, the post-nucleation state is not so simply related to the history where voids have been present from the start since void growth itself has a strong history dependence. Under proportional stressing the following statement quite closely reflects the Gurson model prediction. The deviatoric part of the strain following nucleation of ρ volume fraction of voids is almost the same as the deviatoric strain if the voids were present from the start and had grown to a current void volume fraction ρ. In other words, under proportional stressing, the deviatoric macroscopic strain at a given current void volume fraction ρ is essentially independent of whether the voids were present from the start or whether they were nucleated late in the history.

Conclusions

Relatively small amounts of void nucleation can significantly affect macroscopic hardening behavior. Moreover, the longer nucleation is delayed generally the larger will be its softening contribution. For example, in uniaxial tension from Eq 12 or 13,

$$\dot{\rho}\Delta E_3 = \frac{2}{3}\dot{\rho}F\Sigma_3/E_t \tag{34}$$

if the small dilatational component is neglected. Delaying nucleation increases Σ_3 and decreases E_t, thereby increasing the strain contribution due to nucleation. The tangent modulus of the macroscopic stress-strain curve in the presence of the nucleation, E_t^N, is related to the tangent modulus in the absence of nucleation, E_t, by

$$\frac{1}{E_t^N} = \frac{\dot{E}_3}{\dot{\Sigma}_3} = \frac{1}{E_t}\left[1 + \frac{\dot{\rho}}{\dot{\Sigma}_3}\frac{2}{3}F\Sigma_3\right] \tag{35}$$

Regarding ρ as a function of E_3 and replacing $\dot{\rho}/\dot{\Sigma}_3$ with $(d\rho/dE_3)/E_t^N$, one obtains

$$\frac{E_t^N}{E_t} = 1 - \frac{2}{3}F\frac{d\rho}{dE_3}\frac{\Sigma_3}{E_t} \tag{36}$$

This formula reveals that the macroscopic hardening rate as measured by E_t^N is not only diminished by delayed nucleation, as just discussed, but also by an increased rate of nucleation as measured by $d\rho/dE_3$ and by triaxial effects through F. As discussed by Needleman and Rice [7], the macroscopic hardening rate can become negative at rates of nucleation which are not excessively large. In uniaxial tension, $2F/3$ from the J_2-flow theory calculation is about 2. A typical value of Σ_3/E_t is about 1, in which case E_t^N will be negative if $d\rho/dE_3 \cong$ ½. In other words, a burst of nucleation giving a 1% volume fraction of voids over a 2% range of strain will produce a negative overall strain hardening rate over this range. Such bursts of nucleation are destabilizing, leading to flow localization on the macroscopic scale.

A separate issue which has surfaced in the present study is the unusually strong sensitivity of the predictions to the choice of multiaxial plasticity law for the matrix material, that is, to isotropic or kinematic hardening. The F-factor in Eqs 34 and 36, as computed assuming kinematic hardening, can be as much as two or three times the corresponding value computed assuming isotropic hardening. It is an open question at this point as to which plasticity law gives the more realistic representation of matrix behavior in this application. Based on experience with other applications involving nonproportional stressing where large differ-

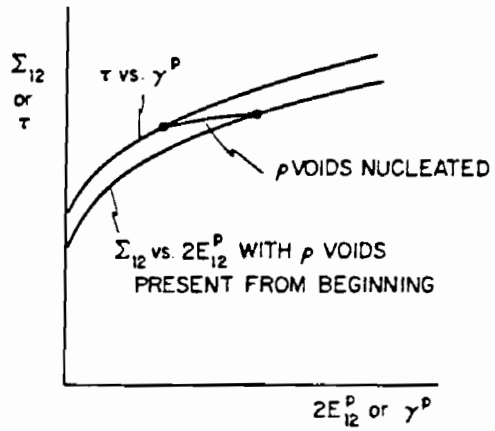

FIG. 16—*Effect of nucleation on shear stress-strain behavior according to Gurson theory.*

ences between predictions on the two plasticity laws are found, the predictions assuming isotropic hardening are likely to underestimate the strain contribution while the kinematic hardening predictions may be more realistic. If so, bursts of nucleation at finite strain are even more destabilizing than one would infer from the Gurson model for example.

The remarkable thing about the kinematic hardening results in Fig. 12 is that at a given stress, the strain subsequent to delayed nucleation is greater than when the void is present from the beginning. This effect seems counterintuitive since even a nonlinear elastic solid would only experience the same strain following delayed nucleation as when the void is present from the start. The effect can be understood only in terms of the nonproportional stressing in the vicinity of the void during nucleation and the reduced resistance to plastic flow associated with the high curvature of the kinematic hardening yield surface.

Acknowledgment

The work of JWH was supported in part by the Materials Research Laboratory under Grant NSF-DMR-83-16979, by the National Science Foundation under Grant NSF-MSM-84-16392, and by the Division of Applied Sciences, Harvard University. The work of VT was supported by the Danish Technical Research Council through Grant 16-4006.M.

APPENDIX

Method for Calculating ΔE

To formulate a minimum principle for the displacement rates, let

$$w(\mathbf{s}, \dot{\boldsymbol{\epsilon}}) = \frac{1}{2}\dot{\sigma}_{ij}\dot{\epsilon}_{ij} \tag{37}$$

be the stress dependent strain-rate potential of the matrix material evaluated using either Eqs 5 and 6 for J_2-flow theory or Eqs 6 and 7 for kinematic hardening theory. For the moment, suppose the void is nucleated in a spherical block of material of radius R (subsequently R will be allowed to become infinite), which is stressed into the plastic range by uniform tractions $\Sigma_{ij}n_j$ applied to its surface A_R, where n is the outward unit normal to A_R. As discussed in the section on Nucleation of an Isolated Void, during nucleation traction rates $-\dot{\lambda}_0 T_i^0$ are applied to the surface A_0 of the unit void being nucleated, simultaneously with traction rates $\dot{\lambda}_\infty \Sigma_{ij}n_j$ applied on A_R. For the finite region with outer radius R, the actual displacement rates minimize

$$W = \int_V w(\mathbf{s}, \dot{\boldsymbol{\epsilon}})\, dV + \dot{\lambda}_0 \int_{A_0} T_i^0 \dot{u}_i\, dA - \dot{\lambda}_\infty \int_{A_R} \Sigma_{ij} n_j \dot{u}_i\, dA \tag{38}$$

where V is the region exterior to A_0 and interior to A_R.

The principle must be modified such that the functional remains bounded when $R \to \infty$. To this end, let $\dot{\boldsymbol{\epsilon}}^\infty$ be the strain rate at infinity associated with $\dot{\lambda}_\infty \Sigma_{ij}$ and let $\dot{\mathbf{u}}^\infty$ be a dis-

placement rate field such that

$$\dot{\epsilon}_{ij}^{\infty} = \frac{1}{2}(\dot{u}_{i,j}^{\infty} + \dot{u}_{j,i}^{\infty})$$

Following procedures similar to those given for visco-plastic behavior in Ref 9, one can show that Eq 38 can be replaced by the modified functional of the additional displacement rates

$$W = \int_V [w(\mathbf{s}, \dot{\boldsymbol{\epsilon}}) - w(\mathbf{s}, \dot{\boldsymbol{\epsilon}}^{\infty}) - \dot{\Sigma}_{ij}\dot{\epsilon}_{ij}]\, dV + \int_{A_0} (\dot{\lambda}_{\infty}\Sigma_{ij}n_j + \dot{\lambda}_0 T_i^0)\dot{u}_i\, dA \tag{39}$$

where n points into the void on A_0 and the additional rate quantities are defined by

$$\dot{\tilde{\boldsymbol{\epsilon}}} = \dot{\boldsymbol{\epsilon}} - \dot{\boldsymbol{\epsilon}}^{\infty} \text{ and } \dot{\tilde{\mathbf{u}}} = \dot{\mathbf{u}} - \dot{\mathbf{u}}^{\infty} \tag{40}$$

The modified function is minimized by the actual additional displacement rates. Moreover, the modified functional remains well-conditioned as $R \to \infty$ for all fields for which $\dot{\tilde{\boldsymbol{\epsilon}}}$ decays faster than $r^{-3/2}$.

The desired extra strain contribution, ΔE, due to nucleation of the void is obtained for the *finite problem* by integrating over the nucleation history the incremental contribution

$$\Delta \dot{E}_{ij} = \frac{1}{2}\int_{A_R} (\dot{\tilde{u}}_i^0 n_j + \dot{\tilde{u}}_j^0 n_i)\, dA \tag{41}$$

where $\dot{\tilde{\mathbf{u}}}^0$ is that part of the additional field due to just the traction rate $-\dot{\lambda}_0 T_i^0$ on A_0. As discussed in the section on Nucleation of Isolated Voids, the contribution due to $\dot{\lambda}_{\infty}\Sigma_{ij}n_{ij}$ on A_R is not included. The two contributions to the additional field are easily separated as discussed below. Equation 41 applies for the finite region but cannot be used for the limit solution with $R = \infty$. An alternative means of calculating $\Delta\mathbf{E}$, which does apply in the limit, makes use of the reciprocal theorem and an auxiliary solution. For the auxiliary solution, let $\dot{\Sigma}_{ij}^A n_j$ be applied on A_R with zero traction rates on A_0 and let $\dot{u}_i^A$ be the associated displacement-rate field calculated using the same distribution of the incremental moduli as in the incremental nucleation problem itself. By reciprocity

$$\dot{\Sigma}_{ij}^A \Delta \dot{E}_{ij} = \int_{A_R} \dot{\Sigma}_{ij}^A \dot{\tilde{u}}_i^0 n_j\, dA = -\int_{A_0} \dot{\lambda}_0 T_i^0 \dot{u}_i^A\, dA \tag{42}$$

since $\dot{\tilde{u}}_i^0$ is that part of the solution associated with zero traction rates on A_R. The integral over A_0 in Eq 42 is readily calculated in the limit $R \to \infty$, and the individual components of $\Delta\dot{\mathbf{E}}$ can be computed by making several appropriate choices for $\dot{\boldsymbol{\Sigma}}^A$.

Since the solution has axial symmetry with respect to the x_3-axis, let r and θ be radial and azimuthal coordinates with θ measured from the x_3-axis. The additional velocity fields in the incompressible matrix are generated from a velocity potential according to

$$\dot{\tilde{u}}_r = -r^{-2}(\sin\theta)^{-1}(\Psi \sin\theta)_{,\theta}, \quad \dot{\tilde{u}}_\theta = r^{-1}\Psi_{,r} \tag{43}$$

The velocity potential used in the calculations was

$$\Psi = a_0 \cot \theta + \sum_{k=2,4,\ldots} \sum_{j=1,2,3,\ldots} a_{kj} r^{-j+1} [P_k(\cos \theta)]_{,\theta} \tag{44}$$

where the a's are amplitude factors which were chosen to minimize Eq 39 and $P_k(x)$ is the Legendre polynomial of degree k. The lead term, $a_0 \cot \theta$, is the spherically symmetric contribution.

Denote the set of free amplitude factors by A_i, $i = 1, N$ and introduce the notation

$$\dot{\mathbf{u}} = \sum_{i=1}^{N} \dot{A}_i \mathbf{u}^{(k)}, \quad \dot{\boldsymbol{\epsilon}} = \sum_{i=1}^{N} \dot{A}_i \boldsymbol{\epsilon}^{(k)} \tag{45}$$

The functional (Eq 39) becomes

$$W = \frac{1}{2} \sum_{i=1}^{N} \sum_{j=1}^{N} M_{ij} \dot{A}_i \dot{A}_j + \sum_{i=1}^{N} B_i \dot{A}_i \tag{46}$$

where

$$M_{pq} = \int_V L_{ijkl} \epsilon_{ij}^{(p)} \epsilon_{kl}^{(q)} \, dV \tag{47}$$

and

$$B_p = \int_{A_0} (\dot{\lambda}_\infty \Sigma_{ij} n_j + \dot{\lambda}_0 T_i^0) u_i^{(p)} \, dA + \int_V [L_{ijkl} - L_{ijkl}^\infty] \dot{\epsilon}_{ij}^\infty \epsilon_{kl}^{(p)} \, dV \tag{48}$$

Here $\mathbf{L}$ are the incremental moduli at a given point and $\mathbf{L}^\infty$ are the incremental moduli at infinity. The stress and the incremental moduli are updated at each incremental step of the solution allowing for the possibility of elastic unloading or plastic loading. The equations for the increments of the amplitude factors follow immediately from Eq 46 as

$$\sum_{j=1}^{N} M_{ij} \dot{A}_j = -B_i \quad i = 1, N \tag{49}$$

The volume integrals in Eqs 47 and 48 were evaluated numerically using 10×10 Gauss-type formulas over the domain of r and θ. The surface integrals in Eqs 48 and 42 were evaluated analytically. The auxiliary problem and the problem for $\dot{\mathbf{u}}^0$ are obtained from Eq 49 simply by changing the B-vector. For the auxiliary problem $\dot{\lambda}_\infty \boldsymbol{\Sigma}$ is replaced by $\dot{\boldsymbol{\Sigma}}^A$ and $\dot{\lambda}_0$ is set to zero; for the problem for $\dot{\mathbf{u}}^0$, $\dot{\lambda}_\infty$ (and $\dot{\boldsymbol{\epsilon}}^\infty$) is set to zero. The strain contribution due to nucleation of the void is readily calculated from Eq 42. The calculations for F and G reported in the body of the paper were carried out using the same seven free amplitudes as in Ref 9, corresponding to a_0 and a_{kj} with $k = 2, 4$ and $j = 1, 2, 3$ in Eq 44.

References

[1] Gurson, A. L., *Journal of Engineering Materials and Technology*, Vol. 99, 1977, pp. 2–15.
[2] Needleman, A., "A Continuum Model for Void Nucleation by Inclusion Debonding," *Journal of Applied Mechanics*, Vol. 54, 1987, pp. 525–532.

[3] Hutchinson, J. W. in *Numerical Solution of Nonlinear Structural Problems*, AMD-Vol. 6, R. F. Hartung, Ed., American Society of Mechanical Engineering, 1973, pp. 17–30.
[4] Tvergaard, V., *International Journal of Mechanical Sciences*, Vol. 20, 1978, pp. 651–658.
[5] Tvergaard, V., *Journal of the Mechanics and Physics of Solids*, Vol. 35, 1987, pp. 43–60.
[6] Saje, M., Pan, J., and Needleman, A., *International Journal of Fracture*, Vol. 19, 1982, pp. 163–182.
[7] Needleman, A. and Rice, J. R. in *Mechanics of Sheet Metal Forming*, D. P. Koistinen and N.-M. Wang, Eds., Plenum Publishing Company, New York, 1978, pp. 237–265.
[8] Tvergaard, V., *International Journal of Fracture*, Vol. 18, 1982, pp. 237–252.
[9] Budiansky, B., Hutchinson, J. W., and Slutsky, S. in *Mechanics of Solids*, H. G. Hopkins and M. J. Sewell, Eds., Pergamon Press, New York, 1982, pp. 13–46.